Journal of Bioenergetics and Biomembranes, Vol. 32, No. 5, 2000

Osmomechanics of the *Propionigenium modestum* F_o Motor

Peter Dimroth,[1,2] Ulrich Matthey,[1] and Georg Kaim[1]

In *Propionigenium modestum*, ATP is manufactured from ADP and phosphate by the enzyme ATP synthase using the free energy of an electrochemical gradient of Na^+ ions. The *P. modestum* ATP synthase is a clear member of the family of F-type ATP synthases and the only major distinction is an extension of the coupling ion specificity to H^+, Li^+, or Na^+, depending on the conditions. The use of Na^+ as a coupling ion offers unique experimental options to decipher the ion-translocation mechanism and the osmotic and mechanical behavior of the enzyme. The single *a* subunit and the oligomer of *c* subunits are part of the stator and rotor, respectively, and operate together in the ion-translocation mechanism. During ATP synthesis, Na^+ diffuses from the periplasm through the *a* subunit channel onto the Na^+ binding site on a *c* subunit. From there it dissociates into the cytoplasm after the site has rotated out of the interface with subunit *a*. In the absence of a membrane potential, the rotor performs Brownian motions into either direction and Na^+ ions are exchanged between the two compartments separated by the membrane. Upon applying voltage, however, the direction of Na^+ flux and of rotation is biased by the potential. The motor generates torque to drive the rotation of the γ subunit, thereby releasing tightly bound ATP from catalytic sites in F_1. Hence, the membrane potential plays a pivotal role in the torque-generating mechanism. This is corroborated by the fact that for ATP synthesis, at physiological rates, the membrane potential is indispensable. We propose a catalytic mechanism for torque generation by the F_o motor that is in accord with all experimental data and is in quantitative agreement with the requirement for ATP synthesis.

KEY WORDS: F_1F_o-ATP synthase; F_o motor; intersubunit rotation; membrane potential; torque generation; *Propionigenium modestum.*

INTRODUCTION

A substantial amount of the ATP requirement of living cells is produced by the F_1F_o-type ATP synthases. The majority of these enzymes use an electrochemical proton gradient over the membrane as driving force for ATP synthesis, and hence, the H^+-translocating F_1F_o-ATP synthase of *Escherichia coli* has been studied particularly intensively. Many insightful results on the catalytic mechanism of the F_o motor derived, however, from investigations with the Na^+-translocating F_1F_o-ATP synthase of *Propionigenium modestum.*

Basically, the H^+- and Na^+-translocating F_1F_o-ATP synthases share the same structural and functional principals, the main difference of the *P. modestum* ATP synthase being an extension of the coupling ion specificity from exclusively protons to Na^+, Li^+, or H^+, depending on conditions (Laubinger and Dimroth, 1989; Kluge and Dimroth, 1993a,b). Figure 1 shows the overall geometry of the *P. modestum* ATP synthase. The structure is divided into the membrane-integral F_o moiety, comprising subunits ab_2c_{9-12}, and the peripheral F_1 part, composed of subunits $\alpha_3\beta_3\gamma\delta\varepsilon$. For our purposes, we need only recognize that the entire structure can be subdivided into two counter-rotating assemblies denoted by convention as rotor and stator. The rotor consists of a ring of 9–12 *c* subunits connected to a shaft consisting of the γ and ε subunits. The remainder of the assembly consists of subunits $ab_2\alpha_3\beta_3\delta$ and is the stator. During ATP synthesis, the

[1] Institut für Mikrobiologie, Eidgenössische Technische Hochschule, ETH-Zentrum, CH-8092 Zürich, Switzerland.
[2] To whom all correspondence should be addressed: e-mail: dimroth@micro.biol.ethz.ch

0145-479X/00/1000-0449$18.00/0

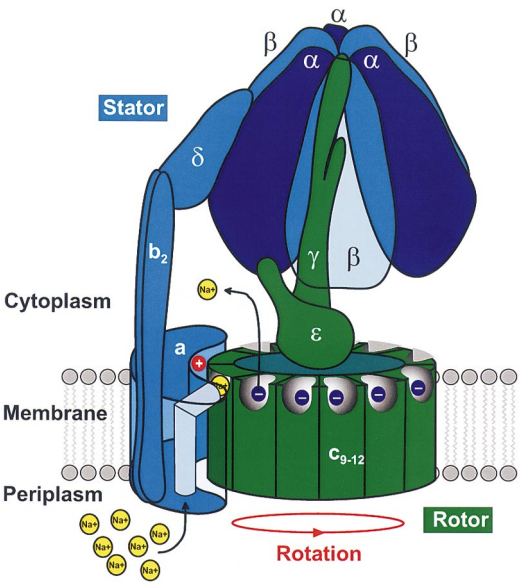

Fig. 1. Illustration showing the structure and function of the *Propionigenium modestum* ATP synthase. The water-soluble F_1 domain with the catalytic sites on the three β subunits is connected via γ and ε subunits with the *c* ring (c_{9-12}) of the F_o domain and via δ and b_2 subunits with the F_o subunit *a*. The rotor (green) consists of subunits $c_{9-12}\ \gamma\varepsilon$ and the stator (blue) consists of subunits $ab_2\alpha_3\beta_3\delta$. The path of Na^+ during ATP synthesis is from the periplasm through the a subunit channel onto an empty *c* subunit site at the rotor–stator interface. After the rotor site has been moved out of the interface with the stator, the Na^+ dissociates into the cytoplasm. The positive stator charge (*a*R227, red), which electrostatically attracts empty, negatively charged rotor sites (*c*E65, dark blue) is indicated.

F_o motor converts the energy stored in a transmembrane electrochemical gradient of Na^+ (or H^+) into rotary torque. This drives the rotation of the γ subunit, eliciting conformational changes in the catalytic β subunits so that tightly bound ATP is released. In its reverse operation, the engine acts as an ATP-driven Na^+ or H^+ pump. Rotation of the γ, ε, and *c*-ring assembly is now driven by the hydrolysis of ATP and this rotation forces Na^+ (or H^+) to pass from the *c* subunit-binding sites through the *a* subunit channel to the periplasmic side of the membrane.

ORGANIZATION OF THE F_o SECTOR

Whereas most of the F_1 sector has been solved by X-ray crystallography to atomic resolution (Abrahams *et al.*, 1994), this type of resolution has not yet been obtained for the F_o sector. Low-resolution electron microscopic and atomic force microscopic images initially suggested a ring like arrangement for the *c* oligomer, with subunits *a* and *b* lying at the periphery of the ring (Birkenhäger *et al.*, 1995; Singh *et al.*, 1996; Takeyasu *et al.*, 1996). The ring structure of the *c* oligomer has recently been confirmed by X-ray crystallography of the yeast ATP synthase (Stock *et al.*, 1999). In this structure, a ring of 10 *c* subunits was attached to the F_1 headpiece via contacts with the γ and ε subunits. The structure is in complete harmony with earlier suggestions that the *c* subunit oligomer is part of the rotor and its rotation has recently been shown by direct visualization (Sambongi

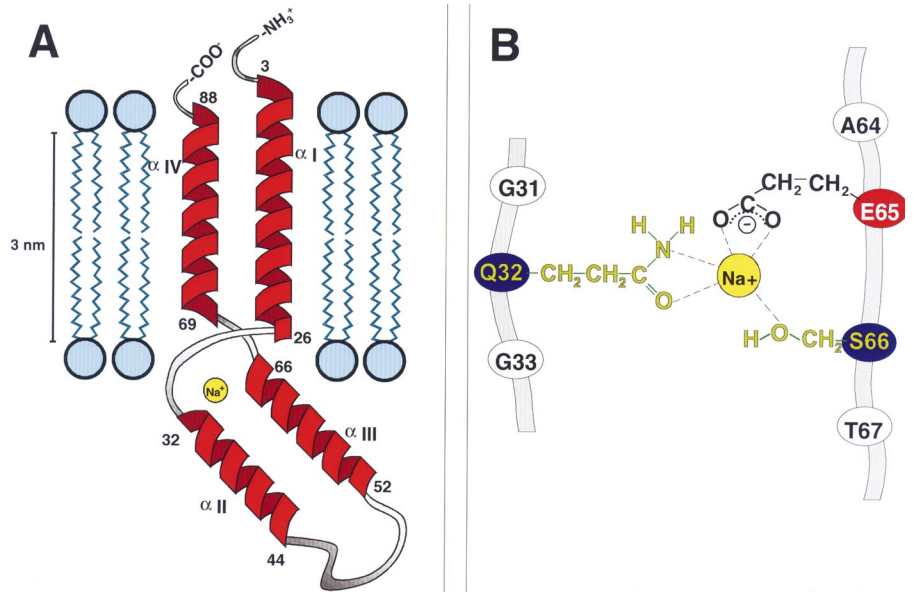

Fig. 2. See legend on facing page.

et al., 1999; Pänke *et al.*, 2000) using the technique originally developed to investigate the rotation of the γ subunit (Noji *et al.*, 1997). In another report, however, the techniques used to visualize the rotation of the *c* oligomer have been challenged (Tsunoda *et al.*, 2000). During the rotation of the rotor subunits γ, ε, and the *c* ring in the center of the molecule, the stator subunits must stick together, and there is evidence that the *a* subunit located within the membrane peripheral to the *c* ring is connected via an extended *b* dimer to the outside of the $\alpha_3\beta_3$ cylinder using subunit δ as a linker (Rodgers and Capaldi, 1998; Dunn and Chandler, 1998).

The stoichiometry of *c* subunits in the oligomer may vary among species: while 10 copies can be counted in the X-ray structure of the yeast enzyme (Stock *et al.*, 1999) and 14 copies are seen in atomic force microscopy of the chloroplast ATPase (Seelert *et al.*, 2000), 12 *c* subunits have been suggested to form the ring in the *E. coli* ATP synthase (Fillingame *et al.*, 2000). Exceptionally stable *c* subunit assemblies are present in the ATP synthases from *P. modestum* (Laubinger and Dimroth, 1988) or *Ilyobacter tartaricus* (Neumann *et al.*, 1998), in which even boiling with sodium dodecyl sulfate (SDS) is not sufficient to dissociate the complex into monomers. The unusual stability of the *c* subunit oligomer in the presence of SDS is one of the reasons to believe that SDS does not lead to a complete unfolding of monomeric subunit *c* (see below). Monomeric subunit *c* is conveniently isolated from whole cells by extraction with chloroform/methanol and fractionation on an ion-exchange column in mixed organic solvents. Subunits *c* from different species contain only 75–90 amino acid residues and, therefore, structure determination by nuclear magnetic resonance (NMR) is feasible.

Structure determination of *P. modestum* subunit *c* by the NMR method was performed with dodecyl sulfate micelles because dodecyl sulfate did not affect the stability of the *c* subunit oligomer (see above). It was, therefore, unlikely that dodecyl sulfate led to a significant unfolding of the molecule. Furthermore, nativelike folding of a membrane protein might be more readily expected in detergent micelles mimicking more closely the biphasic character of the membrane than in an organic solvent mixture, which is monophasic. A single molecule of subunit *c* was dispersed into one dodecyl sulfate micelle (Matthey *et al.*, 1999). The secondary structure of the protein was highly α-helical and rather robust, not changing upon heating to 60°C, as shown by circular dichroism (CD) spectroscopy (Matthey *et al.*, 1997). A nativelike folding of subunit *c* in dodecyl sulfate micelles was indicated by dicyclohexylcarbodiimide (DCCD) labeling experiments. About 60% of the *c* subunits were modified during a 15-h incubation with the reagent (unpublished results). Although the initial rate of the modification reactions was approximately two orders of magnitude lower than in the F_1F_o complex, the similarity of the pH profile and the specific protection by Na^+ from the reaction with DCCD provide important evidence for a nativelike folding of monomeric subunit *c* in dodecyl sulfate micelles. Furthermore, these data indicate that Na^+ binds to a monomeric *c* subunit, thereby protecting it from the modification with DCCD. The presence of a Na^+ binding site within an individual *c* subunit is in contrast to suggestions made by Fillingame and colleagues that twin *c* subunits are required to create a Na^+ binding site (Dmitriev *et al.*, 1999).

The secondary structure of *P. modestum* subunit *c* in dodecyl sulfate micelles was well defined by the NMR data (Matthey *et al.*, 1999), but due to the lack of clearly defined long-range NOE's, it was not possible to resolve the structure in its tertiary fold. *Propionigenium modestum* subunit *c* folds into four clearly defined α-helices connected by short peptides with nonregular secondary structures. The N-terminal helix (I, 23 residues) and the C-terminal helix (IV, 19 residues) were proposed to span the membrane, and the additional helices II (12 residues) and III (14 residues) and the intervening hydrophilic loop (8 residues) were proposed to protrude into the cytoplasm (Fig. 2A). In this structure, the Na^+ binding residues Q32, E65, and S66 (Fig. 2B) (Kaim *et al.*, 1997) are located in the helix I $\rightarrow$ II and helix III $\rightarrow$ IV connections, probably near the membrane surface on the cytoplasmic side. Hence, direct cytoplasmic access of these sites is readily conceivable in accord with several lines of experimental evidence obtained with the ATP synthase of *P. modestum* (Kaim and Dimroth, 1998).

The structure of *E. coli* subunit *c* has been determined by NMR in a chloroform–methanol–water (4:4:1) solvent mixture at pH 5.0 and 8.0 (Girvin *et al.*, 1998; Rastogi

Fig. 2. (A) Model for insertion of *Propionigenium modestum* subunit *c* into the membrane. Helices I (αI; 24 residues) and IV (αIV; 18–20 residues) span the membrane; helices II (αII; 13 residues) and III (αIII; 15 residues) and the connecting loop of seven amino acid residues are exposed to the cytoplasm. The Na^+ binding site is located in the region of irregular secondary structure between helices I and IV and helices II and III and comprises residues of the N-terminal as well as the C-terminal sections of the polypeptide chain (Q32, E65, S66). The Na^+ binding site lies near the cytoplasmic membrane surface. This location is in accord with biochemical data indicating free access of this site for Na^+ from the cytoplasm. (B) Details of the Na^+ coordination sphere with ligands contributed by Q32, E65, and S66. Only residues E65 and S66 are required for Li^+ binding; E65 is the only residue required for H^+ binding and translocation.

and Girvin, 1999). At both pH values, monomeric subunit *c* folds into two extended α-helices of 38 and 33 residues, respectively, which closely associate with one another, and a short intervening hydrophilic loop. The main difference in the structures at the different pH values is a 140° twist of helix II versus helix I connected with structural changes in the loop. The structures have been modeled into the membrane such that D61, which is the equivalent of E65 of *P. modestum* and, therefore, involved in the ion-translocation mechanism, became positioned in the center of the bilayer (Fillingame *et al.*, 2000). Such a position has severe consequences on the potential ion-translocation mechanism and proposals have been made that are heavily based on this modeling of the structure into the membrane. One of the consequences is that D61 cannot be accessible from the cytoplasmic surface without the help of an access channel and, as another consequence, D61 for electrostatic reasons must always be protonated while being in contact with the bilayer and can only deprotonate while being in contact with subunit *a*. In a later chapter, we shall come back to the functional models that were based on the membrane-buried location of D61. At this point, it should be indicated, however, that the membrane boundaries of the *c* subunits are unknown and that the two helices could be moved toward the cytoplasm significantly. If the shorter C-terminal helix would insert into the membrane with the C-terminal A79, D61 would be positioned close to the cytoplasmic surface, where it could have direct access to the cytoplasmic reservoir. It should also be emphasized that the cross-linking data obtained for helix II of subunit *c* and helix IV of subunit *a* (Jiang and Fillingame, 1998) are not conceivable with the subunit *c* structure obtained at pH 5.0, but perfectly match the results expected for the pH 8.0 structure. Furthermore, in the pH 5.0 structure I28, which is at the equivalent position to Q32 of *P. modestum* subunit *c*, and D61, which is at the equivalent position to E65 of *P. modestum* subunit *c*, face into different directions, yet Q32 and E65 of *P. modestum* are Na^+ binding ligands and monomeric subunit *c* binds Na^+ (Kluge and Dimroth, 1994; Matthey *et al.*, 1997). Interestingly enough, I28 and D61 of *E. coli* subunit *c* are facing the same surface in the pH 8.0 structure. One would, therefore, be inclined to speculate that the pH 8 structure more closely resembles the structure of subunit *c* in its native environment. Changes of pH are well known to affect the structure of a protein and decreasing the pH from 8.0 to 5.0 may not only protonate D61, but other acidic amino acids as well. As long as there are no explicit data that show that the structural changes seen in going from the high to the low pH are specifically connected to the protonation of D61 rather than by other amino acids, it seems premature to build a functional model that is based on the two different structures. Other candidate amino acids which might cause the structural changes observed upon protonation are E37 and D44, within the loop region, that may interact differently in the protonated or deprotonated state with the nearby R41 or R50 residues. This might lead to major structural changes in the loop region and might cause the observed rotation of the C-terminal versus the N-terminal helix. Hence, the ion-translocation mechanism proposed by Rastogi and Girvin (1999), which is based on the two structures of subunit *c* determined at pH 5.0 and 8.0 and involves the rotation of helix II versus helix I, can only be valid if both subunit *c* structures reflect physiological states of this molecule.

Probably the most important function of subunit *c* is to bind the coupling ions during their translocation across the membrane. For this purpose, each subunit *c* contains a binding site that specifically recognizes the coupling ion(s). These features were first discovered for *P. modestum* subunit *c* which may bind Na^+, Li^+ or H^+ (Kluge and Dimroth, 1993a, b, 1994). Ligands for Na^+ binding are provided by Q32, E65, and S66 (Fig. 2B), whereas E65 and S66 are sufficient for Li^+ binding, and H^+ binding depends entirely on E65 (Kaim *et al.*, 1997). Consequently, H^+-specific *E. coli* subunit *c* has D61 at an equivalent position to *P. modestum* E65 and, by mutating residues around D61 to the corresponding ones from *P. modestum*, a Li^+ binding site is created (Zhang and Fillingame, 1995).

Subunit *a* is a very hydrophobic protein predicted to fold into five or six-membrane-spanning α-helices connected by short cytoplasmic and periplasmic loops (Yamada *et al.*, 1996; Jäger *et al.*, 1998; Long *et al.*, 1998; Valiyaveetil and Fillingame, 1998). The only strictly conserved residue is R227 (*P. modestum* numbering) and no substitutions at this position permit ATP synthesis (Cain and Simoni, 1988; Lightowlers *et al.*, 1987). According to the topology of subunit *a*, R227 is located near the cytoplasmic surface (Fig. 3) where its electrostatic interaction with E65 of subunit *c* is likely. Subunit *a* contains almost no polar residues in the center of the membrane, but some helices have a few polar residues in the flanking regions between the center region and the two membrane surfaces. The helices may pack to allow for a water-filled channel in the center that is open to the periplasm and closed on the cytoplasmic side. The areas with polar residues could contribute ion-binding sites to select for the specific permeation of the coupling Na^+, Li^+ or H^+ (H_3O^+) across the channel. The accumulation of negatively charged amino acids in the loops is noteworthy (Fig. 3). At the periplasmic side, these charges may contribute to separating the coupling cations from their anions to guide the former specifically into the mouth of the channel.

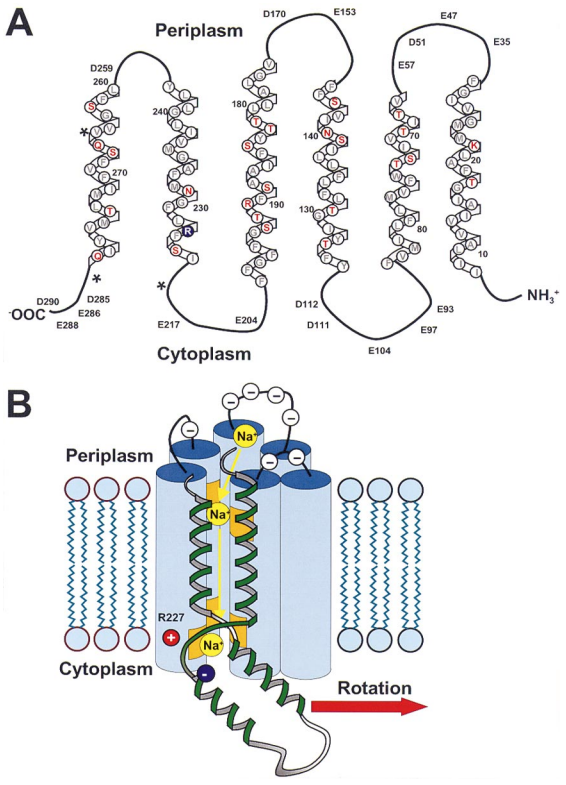

Fig. 3. (A) Sequence and putative topology of subunit a from *Propionigenium modestum*. Negatively charged amino acids are found exclusively in the cytoplasmic and periplasmic loops. The positive stator charge (R227) is in close proximity to the cytoplasmic surface, where it interacts electrostatically with negatively charged rotor sites. Hydrophilic residues in putative transmembrane helices are colored red. The three mutated residues leading to the Na^+ impermeable stator channel are marked (*). (B) Detail of the rotor–stator assembly model as viewed from inside the rotor, showing the *a* subunit (blue cylinders) and a single rotor subunit (green). The location of the essential rotor (dark blue) and stator (red) charges and the path of Na^+ into the stator channel are also indicated. The ion channel terminates before penetrating all the way through the stator. The orange-colored patches indicate polar hydrophilic regions. Rotation during ATP synthesis is to the right.

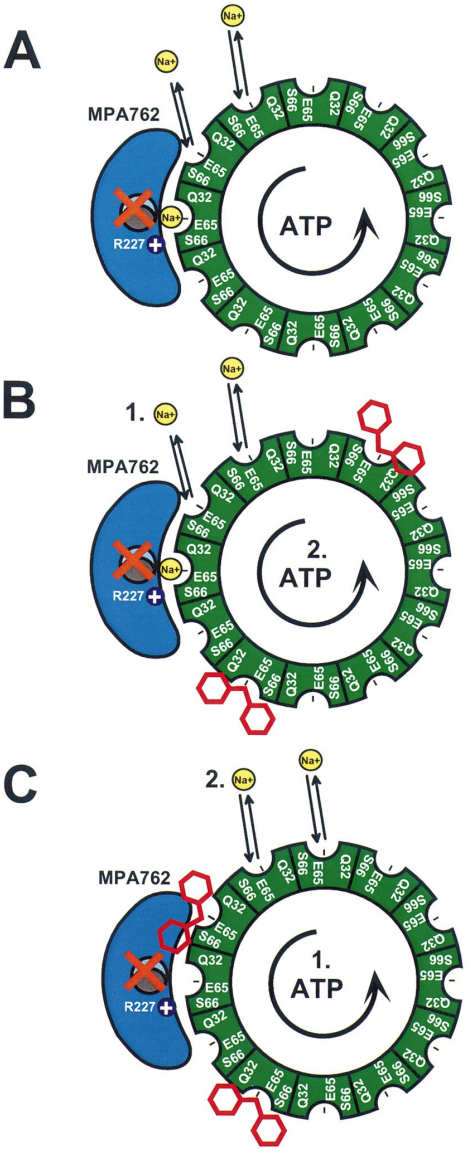

Fig. 4. Illustration showing the occlusion of Na^+ at the interface between a Na^+-binding rotor subunit and the stator a subunit with mutated Na^+-impermeable stator channel. (A) Occlusion of 1 Na^+ per mutant ATP synthase in a strictly ATP-dependent manner. ATP hydrolysis moves a Na^+-boarded rotor site into the interface with the channel. The Na^+ cannot penetrate through this channel due to the mutation and in the Na^+-bound state further ATP-driven rotation is not possible. Therefore the Na^+ is occluded. (B) Na^+ occlusion by the mutant ATP synthase in which part of the rotor sites are modified with DCCD. If Na^+ was added first and ATP second, 1 Na^+ per mutant enzyme was occluded, but if this order was reversed (C), no Na^+ occlusion was observed. Under these conditions, ATP hydrolysis turns the *c* ring with H^+-occupied rotor sites until a DCCD-modified rotor site strikes against the stator and impedes any further rotation. Please note that under the conditions of (B) Na^+ must have direct access to the rotor sites. If Na^+ had to enter the rotor site through an *a* subunit half channel followed by an almost complete revolution to contact the *a* subunit release channel, it would never reach this position due to steric blockade by the DCCD-modified sites in the ring.

INTERACTION BETWEEN SUBUNITS *c* AND *a* IN THE TRANSLOCATION OF COUPLING IONS

Next to the *c* subunits, a crucial role in the ion-translocation mechanism was ascribed to subunit *a*, mainly due to the fact that mutations within this protein affected ATP synthesis or ATP-driven proton pumping to various extents (Cain and Simoni, 1986, 1988, 1989; Lightowlers *et al.*, 1987, 1988; Vik and Antonio, 1994; Valiyaveetil and Fillingame, 1997). R210 of *E. coli* or R227 of *P. modestum* plays a crucial role in the ion-translocation mechanism and all substitutions at this position lead to the complete abolishment of all coupled

ion-transport activities. The fundamental role of subunit *a* in the ion-translocation mechanism has been further corroborated by a family of a subunit mutations of *P. modestum* with alterations of the coupling ion specificity. In the ATPase with the a subunit triple mutation (K220R, V264E, I278N), Na^+ translocation was abolished, but Li^+ or H^+ translocation were retained (Kaim and Dimroth, 1998a). Na^+ ions were not playing a passive role in this mutant, however, but specifically inhibited ATP hydrolysis. This phenotype is in contrast to that of the wild-type enzyme which specifically requires Na^+ ions for its ATPase activity (Laubinger and Dimroth, 1988; Kluge and Dimroth, 1993a). These intricate observations have let us postulate that the reason for the Na^+ inhibition of ATPase activity in the mutant is a blockade in the Na^+ release channel within subunit *a*. This channel would be required to deliver the Na^+ from its subunit *c* binding site at the interface with subunit *a* toward the periplasmic side of the membrane. This hypothesis was verified by $^{22}Na^+$ occlusion experiments (Kaim *et al.*, 1998), the results of which are shown in the illustration in Fig. 4A. One mole of $^{22}Na^+$ was trapped per mole mutant ATPase in a strictly ATP-dependent manner, while no $^{22}Na^+$occlusion was observed under all experimental conditions in the wild-type enzyme. Hence, ATP hydrolysis in the ATPase with the *a* subunit triple mutation is apparently blocked when a Na^+-loaded *c* subunit has been rotated into the interface with the *a* subunit. Here, the Na^+ is entrapped, since the usual exit route through the *a* subunit channel does not allow Na^+ ions to pass to the periplasmic surface and the subunit *c* sites have no access to the cytoplasmic surface as long as they are in contact with subunit *a*. These results show that the ATPase is a perfectly coupled machine where ATP-driven rotation of the *c* ring can only proceed if the Na^+ can be released from the rotor site contacting subunit *a* to the periplasmic side of the membrane. Occlusion of one Na^+ per mutant ATPase is in accord with the one-channel model, predicting free accessibility of all rotor sites of the *c*-subunit ring from the cytoplasm, except those at the interface with subunit *a*. The results are in conflict, however, with the two-channel model that predicts that a rotor site becomes loaded through a cytoplasmic half channel within the *a* subunit and becomes unloaded again through a periplasmic half channel within the *a* subunit after the site has rotated through the bilayer for almost a complete revolution (Junge *et al.*, 1997). This mechanism would imply that the majority of the *c* subunits being in contact with the bilayer are loaded with Na^+ ions and that these Na^+ ions are not accessible to either side of the membrane. Hence, if the two-channel model would be correct, the stoichiometry of occluded Na^+ ions would certainly exceed one and would probably be close to 8–10. Being not in accord with this and many other evidences described below, we regard the two-channel model as an inappropriate description of the F_o mechanism. Further support for the direct accessibility of most of the *c* subunit rotor sites in accord with the one-channel model has been obtained by $^{22}Na^+$ occlusion experiments after modifying part of the rotor sites with DCCD (Fig. 4B, C). $^{22}Na^+$ was again occluded in a 1:1 stoichiometry with the mutant ATPase, but only if $^{22}Na^+$ was added first and ATP second and not if this order of addition was reversed (Kaim and Dimroth, 1998b). In the first case, the occluded Na^+must have entered a site between the modified *c* subunit and subunit *a* and ATP-driven rotation must have stopped after the Na^+-loaded *c* subunit has reached the interface to the *a* subunit. In the second case, however, *c* subunit sites entering the *a* subunit interface by ATP-driven rotation will be filled with protons, not with Na^+. As the protons can be released through the mutated *a* subunit channel, rotation will proceed until a modified rotor subunit strikes against the stator *a* subunit and will be kept there by the torque generated by the F_1 motor. No $^{22}Na^+$ occlusion was observed in the wild-type ATPase. Here, the $^{22}Na^+$-bound rotor sites approaching the wild-type channel release the $^{22}Na^+$ through this channel. This leads to a continued ATP-driven rotation coupled to Na^+ translocation to the periplasmic side of the membrane.

OPERATION PRINCIPLES OF THE F_o MOTOR

Two different operation modes of the F_o motor have been recognized: idling or the generation of torque (Kaim and Dimroth, 1998b). In the idling mode, the rotor performs Brownian back and forth movements against the stator within a narrow angle. This mode is characterized by an exchange of internal and external Na^+ ions and, hence, Na^+ ions have to be present on both sides of the membrane. The idling operation has been discovered during investigations of the isolated F_o motor of *P. modestum* (Kluge and Dimroth, 1992) and it was shown later that the F_o motor also performs idling with the F_1 headpiece attached (Kaim and Dimroth, 1998b). This observation immediately suggested that the angle for the back and forth movement of the rotor should be small, probably between 30° and 60°, because a more substantial rotation of the γ subunit occurring without coupling to ATP synthesis/hydrolysis at the catalytic sites of the β subunits would not be tolerated. Accordingly, after boarding a rotor site from the periplasmic surface through the *a* subunit channel and after rotation out of the rotor/stator interface, the Na^+ has to be released into the cytoplasmic surface before another Na^+ boards the site and rotation goes backward to accommodate $Na^+_{in}/^{22}Na^+_{out}$ exchange. Hence, the Na^{+22}_{in}/Na^+_{out} exchange per se is strong evidence for di-

rectly accessible sites on the rotor outside of the stator interface and is, therefore, not compatible with the two-channel model. This predicts that the rotor sites can only communicate with the two different reservoirs separated by the membrane via two half channels in subunit *a* (Junge *et al.*, 1997). If this model were correct, rotation had to go on for almost a complete revolution (>300°) for a rotor site that was loaded through the access channel with Na^+, in order to release this ion through the release channel into the other reservoir. Even more conclusive is the observation that $Na^+_{in}/^{22}Na^+_{out}$ exchange was not significantly affected by modifying part of the rotor sites of the ring with DCCD. Clearly, this result is to be expected if the one-channel model is valid, but it completely eliminates the two-channel model option: on interrupting the chain of Na^+- carrying rotor sites by the DCCD modification, it would be impossible for a site loaded through the import channel to reach the export channel on subunit *a*. Thus, if we do not want to consider the possibility that the basic structure and mechanism of the F_1F_o-ATP synthases varies among species, all two-channel based models as sophisticated they may be are very probably incorrect (Junge *et al.*, 1997; Rastogi and Girvin, 1999).

It is obvious that the motor has to switch from idling into a torque-generating operation mode in order to perform work. ATP hydrolysis is known to induce torque to the γ subunit and on the rotors extension to the ring of *c* subunits. $Na^+_{in}/^{22}Na^+_{out}$ exchange of the ATPase with partially DCCD-modified *c* subunits was arrested upon ATP addition, but not with ADP or the nonhydrolyzable analog AMP–PNP (Kaim and Dimroth, 1998b). The rotor is apparently turned by the hydrolysis of ATP until a DCCD-modified rotor subunit strikes against the stator subunit where it is kept by the enforced torque in an immobilized position, unable to perform idling and, hence, unable to catalyze $Na^+_{in}/^{22}Na^+_{out}$ exchange.

In the ATP synthesis direction, the electrochemical ion gradient must be the responsible driving force in the torque-generating mechanism. However, surprisingly enough, a Na^+ concentration gradient had no effect on $Na^+_{in}/^{22}Na^+_{out}$ exchange indicating that it is unable to cause the switch from the idling into the torque-generating operation mode (Kaim and Dimroth, 1998b). This highly significant observation has been made for the isolated F_o motor (Kluge and Dimroth, 1992) as well as for the F_o motor attached to the F_1 machinery (Kaim and Dimroth, 1998b). Complementary to this finding, the F_o motor did not catalyze an unidirectional Na^+ ion translocation no matter how large a Na^+ concentration gradient was applied (Kluge and Dimroth, 1992). Based on these observations, one had to assume that the only driving force competent for the switch from idling into torque generation is the membrane potential. Applying a membrane potential of either sign to the reconstituted F_1F_o complex immediately terminated the $Na^+_{in}/^{22}Na^+_{out}$ exchange. Upon applying the potential to the isolated F_o complex, $Na^+_{in}/^{22}Na^+_{out}$ exchange discontinued and, instead, Na^+ flux into the direction of the negative potential was observed. The velocity of unidirectional Na^+ flux was dependent on the eletric potential with very little activity below −40 mV, a midpoint potential around −80 mV, and saturation above −100 mV (Kluge and Dimroth, 1992). It is known that the rotor of the ATP synthase rotates counterclockwise upon ATP hydrolysis if viewed from the periplasm (Noji *et al.*, 1997) and therefore, clockwise rotation should occur during ATP synthesis. Unidirectional Na^+ flux by the isolated F_o motor occurs into the direction of the negative membrane potential (Kluge and Dimroth, 1992) and there are no restrictions for the F_o motor to change its direction of rotation as the membrane potential is reversed. Such restrictions may apply, however, if the F_o sector is connected with F_1 and physiologically, the direction for rotation is determined by the cell's membrane potential, which is positive on the outside.

THE TRANSMEMBRANE ELECTRICAL POTENTIAL IS KINETICALLY INDISPENSABLE FOR THE SYNTHESIS OF ATP

The obligatory role of the membrane potential ($\Delta\Psi$) for switching the motor from an idling into a torque-generating operation mode was highly suggestive for an obligatory requirement of $\Delta\Psi$ in ATP synthesis as well (Kaim and Dimroth, 1998b). With reconstituted proteoliposomes containing the ATP synthase of either *P. modestum*, *E. coli*, or spinach chloroplasts, it has indeed been verified that an ion concentration gradient alone (ΔpNa^+ or ΔpH) was unable to support the conversion of ADP and phosphate into ATP (Kaim and Dimroth, 1999). The rate of ATP synthesis increased exponentially with increasing potentials with midpoint potentials for the *P. modestum* and *E. coli* ATP synthases at around 70 mV and for the chloroplast ATP synthase at around 30 mV. It was also noticed that in the presence of sufficiently high $\Delta\Psi$ values to make the system work, the rate of ATP synthesis was further increased if ΔpNa^+ or ΔpH were applied in addition, but far less than expected if ΔpNa^+ or ΔpH were kinetically equally competent as $\Delta\Psi$. There is no doubt that thermodynamically ΔpNa^+ (or ΔpH) and $\Delta\Psi$ are equivalent and, depending on the conditions, the contribution of ΔpH or ΔpNa^+ as an energy source for ATP synthesis may far exceed that of the $\Delta\Psi$ component. However, for kinetic reasons, the $\Delta\Psi$ component is absolutely essential;

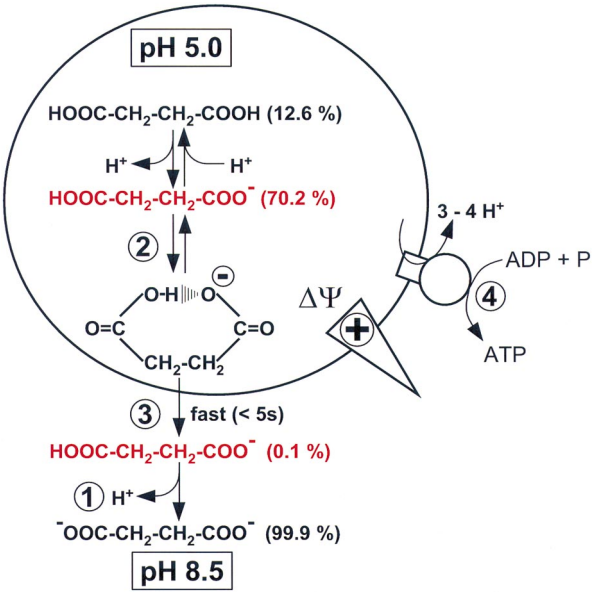

Fig. 5. Generation of a membrane potential by the "acid bath procedure." During the acid stage, the proteoliposomes are equilibrated with 10 mM succinate buffer, pH 5.0. At this pH, 70.2% of the succinate is present as the monoanion. At the basic stage, the external pH is rapidly shifted to pH 8.5 by a 1:1 dilution of the proteoliposome suspension with 100 mM glycylglycine buffer, pH 8.5. This pH jump shifts the equilibrium of external succinate toward the dianion (99.9%), resulting in a large concentration gradient of the succinate monoanion across the membrane (1). The succinate monoanion predominating in the internal compartment, folds partially into a ring. This form is membrane permeable because the negative charge has been delocalized between both carboxylic groups (2). Diffusion of this monoanionic succinate species from the inside to the outside following its concentration gradient generates an electric potential according to the Nernst equation (3). This potential is essential to drive ATP synthesis by proteoliposomes reconstituted, e.g., with the F_1F_o-ATP synthase of chloroplasts (4).

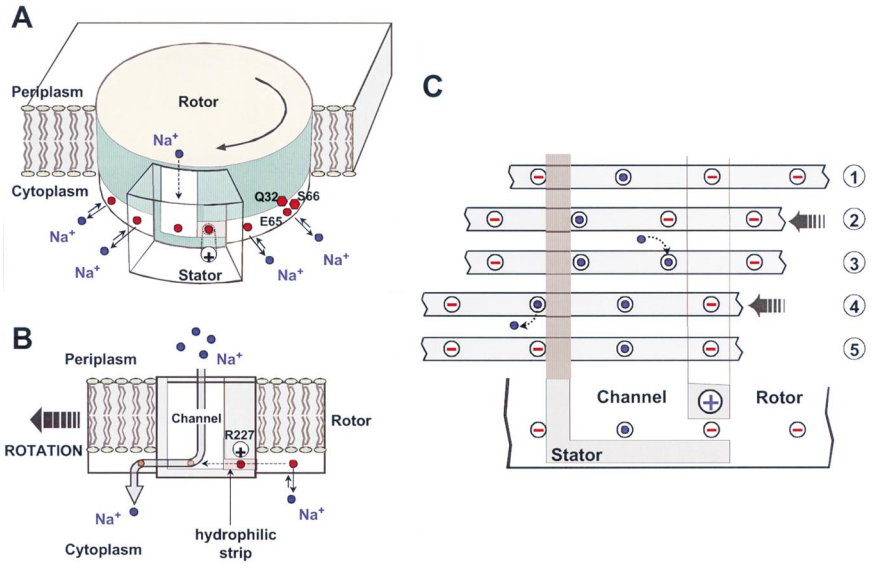

Fig. 6. See legend on facing page.

it guarantees a dramatic increase in the rate of ATP synthesis so that cells can survive. The kinetically indispensable role of the membrane potential for ATP synthesis was completely unexpected, markedly for the chloroplast enzyme, which has been reported to operate on ΔpH alone (Jagendorf and Uribe, 1966). Numerous further studies on this and other ATP synthases seemed to indicate that not only thermodynamically, but also kinetically, ΔpH and ΔΨ are equivalent (Junesch and Gräber, 1991; Turina *et al.*, 1991; Possmayer and Gräber, 1994). Curiously enough, the "acid bath procedure" introduced by Jagendorf and Uribe to generate a ΔpH has been the method of choice for this purpose ever since. An outline of this procedure is shown in Fig. 5. First, the interior volume of the vesicles under investigation was adjusted to pH 4–5 by an incubation with 10 mM succinate buffer of this pH. The pH gradient was then generated by a 1:1 dilution into glycylglycine buffer, pH 8.5. Recently, it has been demonstrated that this method not only established the desired Δ pH but also a ΔΨ of appreciable size due to diffusion of the succinate monoanion (Kaim and Dimroth, 1999). Immediately after the acid–base transition, the concentrations of the succinate monoanion in the acidic interior and the basic exterior are 7.2 and 0.006 mM, respectively. Diffusion of the charged succinate species across the membrane could therefore generate a Nernst potential of 180 mV. This is in reasonable agreement with the ΔΨ of 140 mV determined experimentally. The membrane permeability of the anionic succinate species probably increases significantly upon its folding into a ring in which the negative charge is delocalized to both carboxylic groups. This is in accord with the observation that succinate, maleinate, malate, or malonate, which all can be folded into a ring, are membrane permeable at the pH, where the monoanionic species prevails, whereas fumarate with a *trans* double bond is not. Accordingly, all membrane-permeable dicarboxylic acid monoanions mentioned above, but not fumarate, were able to develop a membrane potential in the acid bath procedure (Kaim and Dimroth, 1999).

TRANSLOCATION OF Na^+ IONS WITH TORQUE GENERATION IN THE F_o MOTOR

Figure 6 shows a model of the *P. modestum* F_o motor that is based on experimental results obtained with this enzyme (Dimroth *et al.*, 1999). The counter-rotating assemblies of the F_o motor make up the rotor consisting of a ring of 9 to 12 copies of subunits *c*, and the stator, comprising subunit *a*. Each rotor subunit contains one Na^+ binding site, consisting of the triad Q32, E65, and S66 near the cytoplasmic surface of the membrane (Kaim *et al.*, 1997). This location allows direct access of the Na^+ ions from the cytoplasmic reservoir to these sites. To prevent ion leakage between the reservoirs, the entire rotor–stator interface is hydrophobic, except for two regions: (1) an ion-selective blind channel within the stator that leads from the periplasm to the level of the rotor sites; and (2) a hydrophilic strip that connects the channel laterally with the cytoplasmic reservoir. This hydrophilic strip provides the assembly with the asymmetry required to induce rotation into a defined direction. The hydrophilic strip permits charged (unoccupied) rotor sites to enter the rotor–stator interface from the right and to pass as far to the left as the edge of the stator channel. The universally conserved positive stator charge (R227) has been placed close to this strip to prevent ions from leaking through this route to the cytoplasm. Having bound an ion from the channel, a rotor site can pass through the hydrophobic barrier and exit the stator, whereupon the site can discharge its ion to the cytoplasm. Hence, the flux of ions is from the periplasm through the stator channel onto an empty rotor site and from there to the cytoplasm after the rotor has turned.

Fig. 6. (A) Schematic diagrams of the rotor–stator assembly of the *Propionigenium modestum* ATP synthase. During ATP synthesis, the rotor turns to the left (clockwise viewed from the periplasm). The rotor section below the level of the membrane contains the Na^+ binding sites consisting of the triad Q32, E65, and S66. The stator contains an aqueons channel that conducts ions from the periplasmic (positive) reservoir to the level of the horizontal hydrophilic strip. The positive stator charge, R227, blocks leakage of ions along this strip to the cytoplasm. (B) Face-on view of the rotor–stator assembly. Rotation during ATP synthesis is to the left. There are four rotor sites near the stator, two within the rotor–stator interface and two adjacent laterally. The stator is penetrated by an aqueous channel that admits ions from the periplasm, but ions can only exit to the cytoplasm by boarding a rotor site and passing through the dielectric barrier forming the left well of the channel. If the occupied site moves to the right, it quickly loses its ion back to the channel when it approaches the positive stator charge, R227. (C) A typical sequence of events that advance the rotor shown in (1). The third side from the left is held by the stator charge. (1) → (2): the rotor fluctuates so that the third (empty) site jumps out of the potential well of the stator charge. This jump is biased by the membrane potential and is helped by the dielectric barrier preventing the first rotor site (empty) from entering the low dielectric medium of the stator. (2) → (3): Once the third rotor site has moved out of the potential well of the stator charge toward the channel, it quickly binds a sodium ion from the periplasmic reservoir. (3) → (4): the positive stator charge pulls the empty fourth rotor site into its potential well. Since the second rotor site is neutralized, it can pass through the dielectric barrier. (4) → (5): once the second rotor site passes out of the stator, its sodium ion quickly dissociates into the cytoplasmic reservoir. Once empty, it cannot go back into the low dielectric rotor–stator interface. (5) is exactly the same state as (1), but shifted to the left by one rotor step. (Adopted from Dimroth *et al.*, 1999.)

Now let us consider how this ion flux is coupled to the generation of rotational torque and what may be the fundamental role of the membrane potential in the torque-generating mechanism. Because of random Brownian motion, the progression of the rotor is stochastic, but as a result of several electrostatic forces, its diffusion is biased to the left (Fig. 6C). Let us start with a rotor site at the right edge of the stator interface. Occupation of this site is in dissociation equilibrium with the cytoplasmic Na^+ concentration. If the site is empty, it is electrostatically attracted with its negatively charged E65 by the positive stator charge R227. The captured site can escape by thermal fluctuations but, without the membrane potential, it is as likely to escape to the right as to the left. If the channel is aqueous, the bulk of the potential drop will be across the hydrophilic strip. This biases the thermal escape of the rotor site from its potential well to the left. Once in contact with the channel, the site will quickly pick up an ion, which reduces its electrostatic field to that of a dipole. This prevents it from being attracted backward by the stator charge and enables it to pass easily through the hydrophobic barrier, when the next site diffuses into the stator and is captured by the stator charge. When the site emerges from the stator, it quickly loses its ion to the cytoplasm. With its negative charge, the site now encounters the dielectric barrier of the stator and cannot diffuse back to the right. Thus, the membrane potential plays the pivotal role in biased diffusion of the rotor to the left and is, hence, essential for the generation of rotary torque. A low Na^+ concentration at the cytoplasmic side accelerates rotation, because most rotor sites are empty and, therefore, attracted more frequently to the stator charge. A high Na^+ concentration on the periplasmic side also accelerates rotation, because an empty rotor site, having escaped from the stator charge to the channel, picks up a Na^+ more quickly, and this favors its progression to the left. It is important to note that Oster and colleagues have made quantitative simulations on the motor's performance using the experimental data obtained from the *P. modestum* ATP synthase (Dimroth *et al.*, 1999). These calculations show that the Na^+ F_o motor generates sufficient torque for ATP synthesis and that almost all of the torque is due to the membrane potential.

REFERENCES

Abrahams, J. P., Leslie, A. G., Lutter, R., and Walker, J. E. (1994). *Nature (London)* **370**, 621–628.

Birkenhäger, R., Hoppert, M., Deckers-Hebestreit, G., Mayer, F., and Altendorf, K. (1995). *Eur. J. Biochem.* **230**, 58–67.

Cain, D. B., and Simoni, R. D. (1986). *J. Biol. Chem.* **261**, 10043–10050.

Cain, D. B., and Simoni, R. D. (1988). *J. Biol. Chem.* **263**, 6606–6612.

Cain, D. B., and Simoni, R. D. (1989). *J. Biol. Chem.* **264**, 3292–3300.

Dimroth, P., Wang, H., Grabe, M., and Oster, G., (1999). *Proc. Natl. Acad. Sci. USA* **96**, 4924–4929.

Dmitriev, O. Y., Jones, P. C., and Fillingame, R. H. (1999). *Proc. Natl. Acad. Sci. USA* **96**, 7785–7790.

Dunn, S. D., and Chandler, J. (1998). *J. Biol. Chem.* **273**, 8646–8651.

Fillingame, R. H., Jiang, W., and Dmitriev, O. Y. (2000). *J. Exp. Biol.* **203**, 9–17.

Girvin, M. E., Rastogi, V. K., Abilgaard, F., Markley, J. L., and Fillingame, R. H. (1998). *Biochemistry* **37**, 8817–8824.

Jagendorf, A. T., and Uribe, E. (1966). *Proc. Natl. Acad. Sci. USA* **55**, 170–177.

Jäger, H. F., Birkenhäger, R., Stalz, W.-D., Altendorf, K., and Deckers-Hebestreit, G. (1998). *Eur. J. Biochem.* **251**, 122–132.

Jiang, W., and Fillingame, R. H., (1998). *Proc. Natl. Acad. Sci. USA* **95**, 6607–6612.

Junesch, U., and Gräber, P. (1991). *FEBS Lett.* **294**, 275–278.

Junge, W., Lill, H., and Engelbrecht, S. (1997). *Trends Biochem. Sci.* **22**, 420–423.

Kaim, G., and Dimroth, P. (1998a). *Biochemistry* **37**, 4626–4634.

Kaim, G., and Dimroth, P. (1998b). *EMBO J.* **17**, 5887–5895.

Kaim, G., and Dimroth, P. (1999) *EMBO J.* **18**, 4118–4127.

Kaim, G., Wehrle, F., Gerike, U., and Dimroth, P. (1997). *Biochemistry* **36**, 9185–9194.

Kaim, G., Matthey, U., and Dimroth, P. (1998). *EMBO J.* **17**, 688–695.

Kluge, C., and Dimroth, P. (1992). *Biochemistry* **31**, 12665–12672.

Kluge, C., and Dimroth, P. (1993a). *Biochemistry* **32**, 10378–10386.

Kluge, C., and Dimroth, P. (1993b). *J. Biol. Chem.* **268**, 14557–14560.

Kluge, C., and Dimroth, P. (1994). *FEBS Lett.* **340**, 245–248.

Laubinger, W., and Dimroth, P. (1988). *Biochemistry* **27**, 7531–7537.

Laubinger, W., and Dimroth, P. (1989). *Biochemistry* **28**, 7194–7198.

Lightowlers, R. N., Howitt, S., Hatch, L., Gibson, F., and Cox, G. (1987). *Biochim. Biophys. Acta* **894**, 399–406.

Lightowlers, R. N., Howitt, S. M., Hatch, L., Gibson, F., and Cox, G. (1988). *Biochim. Biophys. Acta* **933**, 241–248.

Long, J. C., Wang, S., and Vik, S. B. (1998). *J. Biol. Chem.* **273**, 16235–16240.

Matthey, U., Kaim, G., and Dimroth, P. (1997). *Eur. J. Biochem.* **247**, 820–825.

Matthey, U., Kaim, G., Braun, D., Wüthrich, K., and Dimroth, P. (1999). *Eur. J. Biochem.* **261**, 459–467.

Neumann, S., Matthey, U., Kaim, G., and Dimroth, P. (1998). *J. Bacteriol.* **180**, 3312–3316.

Noji, H., Yasuda, R., Yoshida, M., and Kinosita, K., Jr. (1997). *Nature (London)* **386**, 299–302.

Pänke, O., Gumbiowski, K., Junge, W., and Engelbrecht, S. (2000). *FEBS Lett.* **472**, 34–38.

Possmayer, F. E., and Gräber, P. (1994). *J. Biol. Chem.* **269**, 1896–1904.

Rastogi, V. K., and Girvin, M. E. (1999). *Nature (London)* **402**, 263–268.

Rodgers, A. J. W., and Capaldi, R. A. (1998). *J. Biol. Chem.* **273**, 29406–29410.

Sambongi, Y., Itzo, Y., Tanabe, M., Omoto, H., Iwamoto-Kihara, A., Ueda, I., Yanagida, T., Wada, Y., and Futai, M. (1999). *Science* **286**, 1722–1724.

Seelert, H., Poetsch, A., Dencher, N. A., Engel, A., Stahlberg, H., and Müller, D. J. (2000). *Nature (London)* **405**, 418–419.

Singh, S., Turina, P., Bustamante, C. J., Keller, D. J., and Capaldi, R. (1996). *FEBS Lett.* **397**, 30–34.

Stock, D., Leslie, A. G., and Walker, J. E. (1999). *Science* **286**, 1700–1705.

Takeyasu, K., Omote, H., Nettikadan, S., Tokumasu, F., Iwamoto-Kihara, A., and Futai, M. (1996). *FEBS Lett.* **392**, 110–113.

Tsunoda, S. P., Aggeler, R., Noji, H., Kinosita, K., Jr., Yoshida, M., and Capaldi, R. A. (2000). *FEBS Lett.* **470**, 99–104.

Turina, P., Melandri, B. A., and Gräber, P. (1991). *Eur. J. Biochem.* **196**, 225–229.

Valiyaveetil, F. I., and Fillingame, R. H. (1997). *J. Biol. Chem.* **272**, 32635–32641.

Valiyaveetil, F. I., and Fillingame, R. H. (1998). *J. Biol. Chem.* **273**, 16241–16247.

Vik, S. B., and Antonio, B. J. (1994). *J. Biol. Chem.* **269**, 30364–30369.

Yamada, H., Moriyama, Y., Maeda, M., and Futai, M. (1996). *FEBS Lett.* **390**, 34–38.

Zhang, Y., and Fillingame, R. H. (1995). *J. Biol. Chem.* **270**, 87–93.